

Thermometry utilizing stored short-wavelength spin waves in cold atomic ensembles

Xingchang Wang(王兴昌), Jianmin Wang(王建民), Ying Zuo(左瀛), Liang Dong(董亮), Georgios A Siviloglou, and Jiefei Chen(陈洁菲)

Citation: Chin. Phys. B, 2023, 32 (**7**): 074206. DOI: 10.1088/1674-1056/accb4f
Journal homepage: http://cpb.iphy.ac.cn; http://iopscience.iop.org/cpb

What follows is a list of articles you may be interested in

Optical fiber FBG linear sensing systems for the on-line monitoring of airborne high temperature air duct leakage

Qinyu Wang(王沁宇), Xinglin Tong(童杏林), Cui Zhang(张翠), Chengwei Deng(邓承伟), Siyu Xu(许思宇), and Jingchuang Wei(魏敬闯)

Chin. Phys. B, 2022, 31 (**8**): 084204. DOI: 10.1088/1674-1056/ac5889

High sensitivity plasmonic temperature sensor based on a side-polished photonic crystal fiber

Zhigang Gao(高治刚), Xili Jing(井西利), Yundong Liu(刘云东), Hailiang Chen(陈海良), and Shuguang Li(李曙光)

Chin. Phys. B, 2022, 31 (**2**): 024207. DOI: 10.1088/1674-1056/ac0a63

Highly sensitive optical fiber temperature sensor based on resonance in sidewall of liquid-filled silica capillary tube

Min Li(李敏), Biao Feng(冯彪), Jiwen Yin(尹辑文)

Chin. Phys. B, 2019, 28 (**11**): 114201. DOI: 10.1088/1674-1056/ab43be

Investigation and optimization of sampling characteristics of light field camera for flame temperature measurement

Yudong Liu(刘煜东), Md. Moinul Hossain, Jun Sun(孙俊), Biao Zhang(张彪), Chuanlong Xu(许传龙)

Chin. Phys. B, 2019, 28 (**3**): 034207. DOI: 10.1088/1674-1056/28/3/034207

Simulation studies of multi-line line-of-sight tunable-diode-laserabsorption spectroscopy performance in measuring temperature probability distribution function

Zhang Guang-Le (张光乐), Liu Jian-Guo (刘建国), Kan Rui-Feng (阚瑞峰), Xu Zhen-Yu (许振宇)

Chin. Phys. B, 2014, 23 (**12**): 124207. DOI: 10.1088/1674-1056/23/12/124207

Thermometry utilizing stored short-wavelength spin waves in cold atomic ensembles

Xingchang Wang(王兴昌), Jianmin Wang(王建民), Ying Zuo(左瀛), Liang Dong(董亮), Georgios A Siviloglou[†], and Jiefei Chen(陈洁菲)[‡]

Shenzhen Institute for Quantum Science and Engineering and Department of Physics, Southern University of Science and Technology, Shenzhen 518055, *China*

(Received 5 March 2023; revised manuscript received 27 March 2023; accepted manuscript online 7 April 2023)

Temperature, as a measure of thermal motion, is a significant parameter characterizing a cold atomic ensemble optical quantum memory. In a cold gas, storage lifetime strongly depends on its temperature and is associated with the spin wave decoherence. Here we experimentally demonstrate a new spin wave thermometry method relying on this direct dependence. The short-wavelength spin waves resulting from the counter-propagating configuration of the control and the probe laser beams make this thermometry highly suitable for probing *in situ* the atomic motion in elongated clouds as the ones used in quantum memories. Our technique is realized with comparable precision for memories that rely on electromagnetically induced transparency as well as far-detuned Raman storage.

Keywords: optical quantum memory, temperature measurement, collective atomic excitation, electromagnetically induced transparency

PACS: 42.50.Gy, 03.67.Hk, 42.50.Ex, 07.20.Dt **DOI:** 10.1088/1674-1056/accb4f

Quantum repeaters based on laser-cooled atomic ensembles have already shown their potential to act as the entanglement nodes in metropolitan-scale quantum networks.[1,2] For entanglement distribution long storage lifetimes are essential, and therefore the predominant mechanisms of decoherence of the stored spin waves, such as thermal motion and inhomogeneous broadening, must be addressed.

Significant efforts have been made to reduce the decoherence from the inhomogeneous broadening, mainly originating from the uncompensated magnetic fields.[3–5] Extending the storage lifetime limited by the finite momentum of the stored spin waves caused by the unavoidable atomic thermal motion still remains a challenge. An efficient way to solve this problem is to increase the wavelength of the stored spin waves by a colinear arrangement of write and read beams,[6] and such an approach can lead to an extension of the lifetime to the order of milliseconds. However, an inherent limitation of the colinear configuration is the difficulty to avoid the strong scattering from the write/read beams in the Duan–Lukin–Cirac–Zoller scheme,[7] and the control beam in electromagnetically induced transparency (EIT)[8] or the Raman[9] scheme. In all these cases, a small angle is necessary to achieve a trade-off between long storage times and the detrimental effect of the scattering noise.

Therefore, for finite separation angles, lowering the temperature of the atomic ensembles, by slowing down the atomic thermal motion, becomes a necessary step to further improve the storage lifetimes. Confining the atoms in a small volume by an optical dipole trap has led to coherent memories with second-scale lifetimes,[5,10,11] but at the expense of atom number and thus limited optical depth (OD), which is directly related to the storage efficiency.[12] Alternatively, applying sub-Doppler cooling directly to the magneto–optical trap (MOT) loaded atoms, such as polarization gradient cooling (PGC),[13] dark-state cooling[14] can provide a simple and robust way to limit decoherence. In both cases, a precise way to probe the temperature of the atomic ensembles, especially along the photon propagation, is particularly crucial.

The simplest and most commonly used thermometry method for cold atomic ensembles is the time-of-flight (TOF) measurement during which the temperature is determined by the ballistic expansion behavior after the atoms are released from the trap. Several realizations of this technique have been developed over the years including release and recapture,[15] absorption imaging,[16] and fluorescence imaging,[17] among others. In a typical experimental configuration for an atomic quantum memory, the signal beam propagates in the direction of the long axis to utilize the highest available atom number, and thus, maximize its storage efficiency. As a result, the TOF technique can be in that case challenging since cold atomic ensembles have a cylindrical shape with a very high aspect ratio, which makes the necessary times of flight for observing the longitudinal expansion particularly large, and also a nonuniform distribution, which can make the fitting for temperature retrieval less accurate.[18–20]

Several studies have attempted to precisely evaluate the temperature along the stored light propagation direction. The most relevant ones to an atomic quantum memory

[†]Corresponding author. E-mail: siviloglouga@sustech.edu.cn
[‡]Corresponding author. E-mail: chenjf@sustech.edu.cn

© 2023 Chinese Physical Society and IOP Publishing Ltd

rely on probing the spectral profile of the EIT transmission window,[20–22] which has a width associated with thermal motion dephasing. An accompanying limitation is that the spectral width and the level of transparency are very sensitive to the power of the control beam, the overlap of the probe and the control beam, as well as the wavevector mismatch. The idea that enables our thermometry method originates in the realization that the EIT-driven slow and stored light are very sensitive to the atomic motion.[5,6,19]

In this work, we demonstrate a robust thermometry technique to quantify the atomic motion in a cold ensemble based on EIT- and Raman-driven stored light. The decay of short-wavelength spin waves created by a slight deviation from a counter-propagating configuration of the probe/stored and control beams is directly associated to the temperature of the atomic ensemble. While being particularly sensitive to the atomic motion and thus the ensemble temperature, this setup is not affected by the angle fluctuations and the magnetic field-induced inhomogeneous broadening.

Here, we firstly elucidate how the storage lifetime of a short-wavelength spin wave can directly provide the temperature of a thermal gas.[6] A stored spin wave imprinted in an atomic ensemble of N atoms can be described by $|\psi(t)\rangle = S^{\dagger}(t)|g_1,\ldots,g_j,\ldots,g_N\rangle$, where

$$S(t) = \frac{1}{\sqrt{N}}\sum_j \mathrm{e}^{-\mathrm{i}\Delta\boldsymbol{k}\cdot\boldsymbol{r}_j(t)}|g\rangle_j\langle s|$$

is the collective atomic excitation operator.[7] The wavevector of a light-induced spin wave is written as $\Delta\boldsymbol{k} = \boldsymbol{k}_\mathrm{c} - \boldsymbol{k}_\mathrm{p}$, where $\boldsymbol{k}_\mathrm{c}$ and $\boldsymbol{k}_\mathrm{p}$ are respectively the wavevectors of the control and the probe beams of Figs. 1(a)–1(c), and $\boldsymbol{r}_j(t)$ is the position vector of the j-th excited atom.

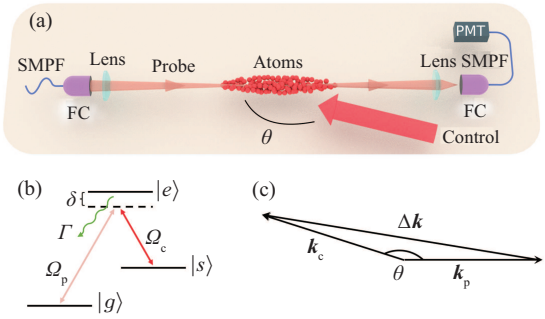


Fig. 1. Experimental setup. (a) Signal probe light beam from a fiber coupler (FC) is focused by a lens to the center of an elongated atomic cloud. A counter-propagating collimated control beam enters the atomic ensemble with a large separation angle θ. The probe beam, after passing from the atoms, is collected by an FC and detected by a photomultiplier tube (PMT) via a single mode polarization-maintaining fiber (SMPF). (b) The three-level scheme for EIT ($|\delta| = 0$) and Raman ($|\delta| \gg \Gamma$) storage. Γ is the decay rate of the excited state $|e\rangle$. (c) The wavevectors $\boldsymbol{k}_\mathrm{c}$ and $\boldsymbol{k}_\mathrm{p}$ of the control and probe beams that determine the spin wave wavelength.

After a storage time τ, the j-th atom, in a collisionless gas, moves to the position $\boldsymbol{r}_j(t+\tau) = \boldsymbol{r}_j(t) + \boldsymbol{v}_j\tau$. The retrieval efficiency η is proportional to the overlap between the final evolution state and the initial one

$$\eta \propto |\langle\psi(t+\tau)|\psi(t)\rangle|^2 = \left|\frac{1}{N}\sum_j \mathrm{e}^{\mathrm{i}\Delta\boldsymbol{k}\cdot\boldsymbol{v}_j\tau}\right|^2 = \left|\int g(\boldsymbol{v})\,\mathrm{e}^{\mathrm{i}\Delta\boldsymbol{k}\cdot\boldsymbol{v}\tau}\,\mathrm{d}\boldsymbol{v}\right|^2, \quad (1)$$

where $g(\boldsymbol{v})$ is the velocity distribution of the atomic ensemble for a continuum approximation. For thermal atoms at temperature T, their motion follows the Maxwell–Boltzmann distribution $g(\boldsymbol{v}) \propto \mathrm{e}^{-m\boldsymbol{v}^2/2k_\mathrm{B}T}$ and after integration over all the possible velocities in Eq. (1), we obtain

$$\eta \propto \mathrm{e}^{-\tau^2/\tau_\mathrm{d}^2}, \quad (2)$$

where $\tau_\mathrm{d} = \lambda/2\pi v_\mathrm{s}$ is the storage lifetime with one-dimensional average velocity $v_\mathrm{s} = \sqrt{2k_\mathrm{B}T/m}$ for atoms with mass m, and k_B is the Boltzmann constant. $\lambda = 2\pi/\Delta k$ is the wavelength of the spin wave. Thus, we derive a simple relation between the storage lifetime and the temperature of the atomic gas

$$\tau_\mathrm{d} = \frac{1}{\Delta k}\sqrt{\frac{m}{2k_\mathrm{B}T}}. \quad (3)$$

In the nearly counter-propagating configuration with a large separation angle θ between the probe and the control beam, the wavevector $\Delta k = k_\mathrm{p} - k_\mathrm{c}\cos\theta \simeq k_\mathrm{p} + k_\mathrm{c}$ of the spin wave corresponds to a very short wavelength compared with the length of the atomic cloud. As is evident from Eq. (3), the spin wave lifetime is impervious to the angle, as shown in Fig. 2, while it is particularly sensitive to the atomic motion and thus appealing for thermometry. For a typical rubidium MOT temperature $T \sim 100$ μK, and an angle $\theta = 178°$, the lifetime is $\tau_\mathrm{d} \approx 0.6$ μs. We note that such lifetimes are intentionally sufficiently short to isolate the contribution of the thermal motion from other common decay mechanisms, such as inhomogeneous broadening decoherence from uncompensated magnetic fields, that are significant in longer time scales. For example, in a 50-mGs (1 Gs $= 10^{-4}$ T) residual magnetic field the estimated lifetime[5] of the stored spin wave is around 100 μs $\gg \tau_\mathrm{d}$.

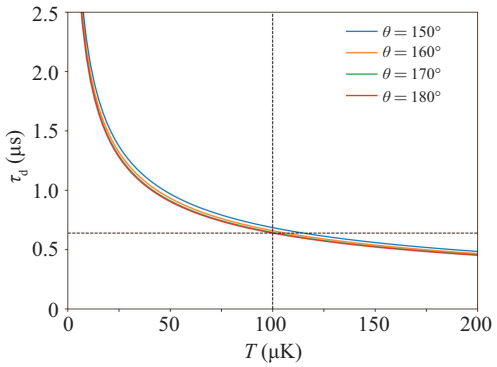


Fig. 2. Theoretical spin wave lifetimes at different angles as a function of temperatures. Evidently, the storage lifetimes are largely insensitive for a wide range of separation angles θ. The dashed lines show how the temperature in a typical rubidium MOT is uniquely determined by the storage lifetime.

In our experiment, more than 10^9 ^{85}Rb atoms are loaded in a two-dimensional MOT created in an ultrahigh vacuum glass cell. Three pairs of counter-propagating, with opposite circular polarizations, trapping beams come from a tapered amplifier seeded by an external cavity diode laser (ECDL). Two repumping beams, along the horizontal and vertical directions, covering the whole atomic cloud are also derived from an ECDL, and they have the same Gaussian profile as the trapping beams. To increase the atomic density and, consequently, the storage efficiency, we implement a dark-line MOT by imaging a wire with a $4f$-configuration on both repumping beams. A racetrack-shaped coil in anti-Helmholtz configuration generates a zero magnetic field line along the long MOT axis and as a result the trapped atomic cloud is cigar-shaped with a length of approximately 2.5 cm and a transverse e^{-2} diameter of 0.54 mm. The magnetic field gradient is switched off 1.5 ms before the trapping beams and remains off for a total of 3.2 ms. The trapping beams stay on for another 1.0 ms and their frequency and power are varied by an acousto–optic modulator (AOM), in order to cool atoms further by PGC. An extra 0.3 ms of trapping beam illumination after the repuming light switched off is applied to initialize all the atoms to the $|5S_{1/2}, F = 2\rangle$ ground state. The experimental cycle has a repetition rate of 50 Hz and it is synchronized with the 220-V AC power.

Probe and control beams come from the same ECDL locked at the crossover transition between $|5S_{1/2}, F = 3\rangle \rightarrow |5P_{1/2}, F = 2\rangle$ and $|5S_{1/2}, F = 3\rangle \rightarrow |5P_{1/2}, F = 3\rangle$. The frequency of the probe beam is upshifted 3.217 GHz by an AOM to be on resonance with the transition $|5S_{1/2}, F = 2\rangle \rightarrow |5P_{1/2}, F = 3\rangle$. The frequency of the coupling beam is shifted by +181 MHz to be on resonance with the transition $|5S_{1/2}, F = 3\rangle \rightarrow |5P_{1/2}, F = 3\rangle$. The probe beam has a power of 200 nW and is focused to an e^{-2} radius of $r_p = 125$ μm at the center of the MOT, and it is collected by a coupling lens to a fiber before detection by a photomultiplier tube (PMT) on the opposite side of the cigar-shaped atomic cloud as shown in Fig. 1(a). The control beam with 1-mW power, is approximately counter-propagating, spatially separated with an angle of 178° with respect to the probe beam, and collimated with a radius of $r_c = 600$ μm, which is wide enough to cover the whole atomic cloud.

The temporal profile of the probe and control beams is amplitude modulated to a Gaussian pulse shape of approximately 1-μs full width at half maximum (FWHM) by an AOM, with a time delay that maximizes the conversion efficiency of the probe light to the stored spin wave. After the storage time, a second control pulse with the same power as the initial one and a pulse width of 10 μs is applied to retrieve the stored spin wave by converting it back to a light pulse with the same wavelength as the probe beam, and is detected by the PMT.

As illustrated above, the lifetime of a short-wavelength spin wave is sensitive to the thermal motion, and therefore can be used to determine the temperature of the atomic medium. To control the temperature in a systematic way, we vary the driving radio frequency (RF) of the trapping laser AOM to change its frequency detuning Δ with respect to the atomic transition $|5S_{1/2}, F = 3\rangle \rightarrow |5P_{3/2}, F = 4\rangle$ from −20 MHz to −35 MHz with a 5-MHz step size as well as the power of the trapping beams.

We record the retrieved signal pulses with an oscilloscope working in average mode for 128 traces. The time separation between each retrieval point is 100 ns, and the full duration of each measurement is 4 μs. To determine the storage efficiency, we integrate the area of the output light signal pulse and normalize it to the corresponding input pulse for each measurement. The measured temporal decay of the probe light converted to spin waves, and the gas temperature, as determined from Eq. (3), are shown in Figs. 3(a) and 3(b).

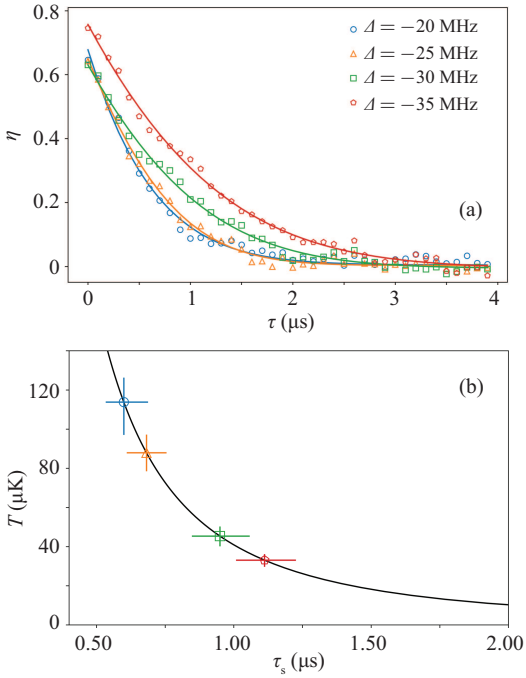


Fig. 3. Thermometry for the EIT scheme. (a) Retrieval efficiency of the stored spin waves as a function of time for different cooling light detunings that correspond to different temperatures. The points are experimental data and the curves are least-squares fits. (b) Calculated temperatures from the measured spin wave $1/e$ lifetimes τ_s. The temperature calibration solid curve is based on the assumption that the lifetime and temperature still follow the relation of Eq. (3) for a separation angle 178°.

For the on-resonance EIT scheme ($|\delta| = 0$), the lifetime decays when the detuning is decreased, and the resulting temperatures increase, as shown in Fig. 3(a), but with a slightly faster rate than expected. To achieve an accurate fitting with the experimental data, an amendment of Eq. (2) is required since the resonant probe pulse experiences a slow light effect with strong re-absorption[19] especially for our large optical depth OD ≈ 300, which is essential for sufficiently high storage efficiency. To phenomenologically model the slow

light effect and other mechanisms related with homogeneous broadening decoherence we multiply the decay function with $e^{-\tau/\tau_\gamma(T)}$, where $\tau_\gamma(T) \propto 1/\sqrt{T}$ is the spin wave relaxation time. Other potential mechanisms that can lead to exponential decays include thermal motion induced Doppler detuning, and leakage of control light during the storage which can introduce dynamic populations in the excited sate with a spontaneous emission loss.[23,24] The extracted temperatures for the various measured storage lifetimes of the EIT are shown in Fig. 3(b).

For the off-resonance Raman scheme ($|\delta| \gg \Gamma$), the aforementioned complications are much less relevant and a clear Gaussian trend is observed (Fig. 4(a)). We avoid the strong re-absorption effect and the control leakage induced loss by shifting the frequency of the probe and control fields by δ. The atomic medium is practically transparent to the probe signal which is absorbed only when it is in two-photon resonance with the control light. The extracted temperatures for the various measured storage lifetimes of the Raman scheme are shown in Fig. 4(b). For both schemes we extract the $1/e$ lifetime $\tau_s(T)$ of the stored spin wave from a general decay function of the form $\eta \propto e^{-\tau^2/\tau_d(T)^2} e^{-\tau/\tau_\gamma(T)}$.[25,26]

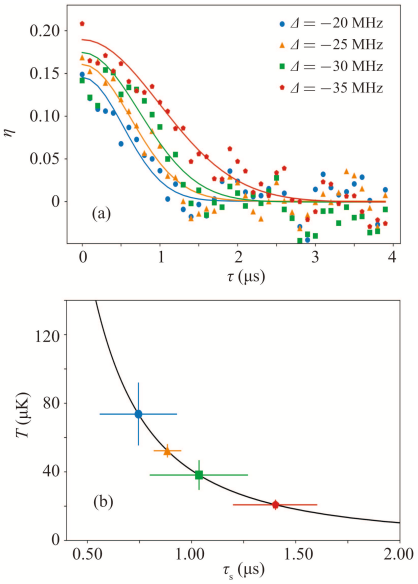


Fig. 4. Thermometry for the Raman scheme. (a) Retrieval efficiency of the stored spin waves as a function of time for different cooling light detunings. The points are experimental data and the curves are least-squares fits. (b) Calculated temperatures from the measured spin wave lifetimes. The solid curve is based on the relation of Eq. (3) for $\theta = 178°$.

In Table 1, all our thermometry results together with estimations from TOF along the transverse directions are given. We note that for such an elongated ensemble the longitudinal temperatures cannot be reliably measured by TOF, mainly because of the need of long falling times for appreciable expansion and the distribution inhomogeneity. The difference in the temperatures along the long axis measured by the storage-based schemes compared with the ones from TOF, which is used for the transverse directions, can be attributed to the absence of magnetic field gradient along z, which can affect the relevant velocity distribution. We note that different temperatures along the radial and axial directions are observed in transverse cooling, Zeeman slowing, and even when the velocity distribution of a fully thermalized gas is filtered by a tube.[27] Our thermometry method qualitatively reproduces the results of the well-established TOF method, while both the EIT- and Raman-driven spin wave schemes provide quantitative information on the temperatures on the longitudinal direction. Excluding the day-to-day system parameters fluctuation, the mismatch may come from the cooling effect in different directions of the atomic cloud. Furthermore, the EIT-created spin wave gives systematically a higher temperature compared to the Raman-driven spin wave and the TOF result, because of the probe absorption and the control leakage induced decay mechanism. In the high temperature regime, the relation curve between storage lifetime and temperature has a low gradient and consequently gives a large temperature disparity in this side. It is also remarkable that our method is expected to achieve higher precision in low temperature regime since the lifetime–temperature curve is exceptionally steep and feasible even in the sub-microKelvin regime where storage in a dipole trap-loaded ultracold atomic gas has been explored.[28,29]

Table 1. Temperatures extracted from three different measurement schemes. The uncertainties of the EIT and the Raman methods are given by least-squares fitting, while the standard deviation of the TOF method is determined by multi-shot measurements of atomic expansion along the transverse direction.

T (μK)	Δ (MHz)			
	−20	−25	−30	−35
EIT	114(15)	88(9)	45(5)	33(3)
Raman	74(18)	52(4)	38(9)	21(3)
TOF	92(12)	63(13)	20(2)	18(5)

In conclusion, we experimentally demonstrated an EIT- and a Raman-driven short-wavelength spin wave thermometry for a counter-propagating configuration of the probe and control light beams. This method relies on the direct relation between the lifetime of the spin wave and the atomic thermal motion, *i.e.*, temperature. Its robustness to misalignment and residual magnetic field fluctuations are also shown. The relative short lifetimes resulting from the short spin wave spatial wavelength are beneficial for thermometry since most of the other decoherence mechanisms act in longer time scales. The EIT method is suitable for lower OD with weak re-absorption and high conversion efficiency while for higher OD case, the Raman method is more reliable and the relatively low conversion efficiency of the Raman spin wave can be improved by simply increasing the power of control field. For a quantum memory, the decoherence mainly comes from the atomic motion along the major axis on which the signal light propagates

and thus our results enable precise probing of this mechanism and benefit memory-based system optimization.[30] Measuring the temperature in the long axis of a laser-cooled atomic ensemble *in situ* can complement the standard TOF method. This new thermometry method can be applied not only to free-space laser-cooled atoms, but also other physical systems that support optical storage like atoms trapped in the nanophotonic structures,[31] rare earth ion crystals,[32] and diamond vacancy centers.[33]

Data availability statement

The data that support the findings of this study are openly available in Science Data Bank at the following link: https://doi.org/10.57760/sciencedb.j00113.00099.

Acknowledgments

Project supported by the National Natural Science Foundation of China (Grant Nos. 12074171, 12074168, 92265109, and 12204227), the Key Laboratory Fund from Guangdong Province, China (Grant No. 2019B121203002), and the Natural Science Foundation of Guangdong Province, China (Grant Nos. 2022B1515020096 and 2019ZT08X324).

References

[1] Yu Y, Ma F, Luo X Y, Jing B, Sun P F, Fang R Z, Yang C W, Liu H, Zheng M Y, Xie X P, Zhang W J, You L X, Wang Z, Chen T Y, Zhang Q, Bao X H and Pan J W 2020 *Nature* **578** 240
[2] Luo X Y, Yu Y, Liu J L, Zheng M Y, Wang C Y, Wang B, Li J, Jiang X, Xie X P, Zhang Q, Bao X H and Pan J W 2022 *Phys. Rev. Lett.* **129** 050503
[3] Katz O and Firstenberg O 2018 *Nat. Commun.* **9** 2074
[4] Xu X T, Wang Z Y, Jiao R H, Yi C R, Sun W and Chen S 2019 *Rev. Sci. Instrum.* **90** 054708
[5] Zhao R, Dudin Y O, Jenkins S D, Campbell C J, Matsukevich D N, Kennedy T A B and Kuzmich A 2009 *Nat. Phys.* **5** 100
[6] Zhao B, Chen Y A, Bao X H, Strassel T, Chuu C S, Jin X M, Schmiedmayer J, Yuan Z S, Chen S and Pan J W 2009 *Nat. Phys.* **5** 95
[7] Duan L M, Lukin M D, Cirac J I and Zoller P 2001 *Nature* **414** 413
[8] Fleischhauer M and Lukin M D 2000 *Phys. Rev. Lett.* **84** 5094
[9] Nunn J, Walmsley I A, Raymer M G, Surmacz K, Waldermann F C, Wang Z and Jaksch D 2007 *Phys. Rev. A* **75** 011401
[10] Dudin Y O, Li L and Kuzmich A 2013 *Phys. Rev. A* **87** 031801
[11] Yang S J, Wang X J, Bao X H and Pan J W 2016 *Nat. Photon.* **10** 381
[12] Gorshkov A V, André A, Fleischhauer M, Sørensen A S and Lukin M D 2007 *Phys. Rev. Lett.* **98** 123601
[13] Vernaz-Gris P, Huang K, Cao M, Sheremet A S and Laurat J 2018 *Nat. Commun.* **9** 363
[14] Rosi S, Burchianti A, Conclave S, Naik D S, Roati G, Fort C and Minardi F 2018 *Sci. Rep.* **8** 1301
[15] Chu S, Hollberg L, Bjorkholm J E, Cable A and Ashkin A 1985 *Phys. Rev. Lett.* **55** 48
[16] Davis K B, Mewes M O, Andrews M R, van Druten N J, Durfee D S, Kurn D M and Ketterle W 1995 *Phys. Rev. Lett.* **75** 3969
[17] Lett P D, Watts R N, Westbrook C I, Phillips W D, Gould P L and Metcalf H J 1988 *Phys. Rev. Lett.* **61** 169
[18] Vengalattore M, Conroy R S and Prentiss M G 2004 *Phys. Rev. Lett.* **92** 183001
[19] Su S W, Chen Y H, Gou S C, Horng T L and Yu I A 2011 *Phys. Rev. A* 83 013827
[20] Peters T, Wittrock B, Blatt F, Halfmann T and Yatsenko L P 2012 *Phys. Rev. A* **85** 063416
[21] Carvalho P R S, de Araujo L E E and Tabosa J W R 2004 *Phys. Rev. A* **70** 063818
[22] dos Santos F B M and Tabosa J W R 2006 *Phys. Rev. A* 73 023422
[23] Wen R, Zou C L, Zhu X, Chen P, Ou Z Y, Chen J F and Zhang W 2019 *Phys. Rev. Lett.* **122** 253602
[24] Wang X, Wang J, Ren Z, Wen R, Zou C L, Siviloglou G A and Chen J F 2022 *Phys. Rev. Lett.* **128** 083605
[25] Shi S, Ding D S, Zhang W, Zhou Z Y, Dong M X, Liu S L, Wang K, Shi B S and Guo G C 2017 *Phys. Rev. A* **95** 033823
[26] Davidson O, Yogev O, Poem E and Firstenberg O 2022 arXiv: 2212.04263
[27] Metcalf H J and van der Straten P 1999 *Laser Cooling and Trapping* (New York: Springer)
[28] Schmidt-Eberle S, Stolz T, Rempe G and Dürr S 2020 *Phys. Rev. A* **101** 013421
[29] Saglamyurek E, Hrushevskyi T, Rastogi A, Cooke L W, Smith B D and LeBlanc L J 2021 *New J. Phys.* **23** 043028
[30] Su K, Wang Y, Zhang S, Kong Z, Zhong Y, Li J, Yan H and Zhu S L 2021 *Chin. Phys. Lett.* **38** 094202
[31] Corzo N V, Raskop J, Chandra A, Sheremet A S, Gouraud B and Laurat J 2019 *Nature* **566** 359
[32] Ortu A, Holzäpfel A, Etesse J and Afzelius M 2022 *npj Quantum Information* **8** 29
[33] Sukachev D D, Sipahigil A, Nguyen C T, Bhaskar M K, Evans R E, Jelezko F and Lukin M D 2017 *Phys. Rev. Lett.* **119** 223602